

The behaviour of a trickle tower electrolytic cell for the production of cobalt(III) acetate from cobalt(II) acetate

U. BAKIR OGUTVEREN*

Anadolu Universitesi, Kimya Muh, Bolumu, 26470 Eskisehir, Turkey

R. E. PLIMLEY

Chemical Engineering Department, University of Newcastle upon Tyne, NE1 7RU, Great Britain

I. NIEVA

Departamento de Industrias, Universidad de Buenos Aires, Argentina

Received 19 February 1991; revised 22 July 1991

The production of Co(III) acetate from Co(II) acetate using a bipolar trickle tower of graphite Raschig rings was investigated. Space time yields up to $18 \text{ kg m}^{-3} \text{ h}^{-1}$ were obtained, which showed no improvement over those achievable in a conventional plate and frame cell. A mathematical model of the system indicated that the electrode reactions occurred almost entirely at the opposing annular surfaces between consecutive layers of Raschig rings and that the unexpectedly low performance of the device was most probably due to the unfavourable mass transport conditions which existed in the intervening gaps.

Nomenclature

a	annular cross sectional area of one Raschig ring (m^2)	I	rings in a vertical row
b_C	kinetic exponential constant for reduction of Co(III) (V^{-1})	k_C	current per vertical column of rings (A)
b_A	kinetic exponential constant for oxidation of Co(II) (V^{-1})	k_C	rate constant for reduction of Co(III) (A m mol^{-1})
b_H	kinetic exponential constant for hydrogen evolution (V^{-1})	k_A	rate constant for oxidation of Co(II) (A m mol^{-1})
b_O	kinetic exponential constant for oxygen evolution (V^{-1})	k_H	rate constant for hydrogen evolution (A m^{-2})
[Co(II)]	concentration of Co(II) (mol m^{-3})	k_O	rate constant for oxygen evolution (A m^{-2})
[Co(III)]	concentration of Co(III) (mol m^{-3})	k_L	mass transfer coefficient (m s^{-1})
F	Faraday constant (96487 C mol^{-1})	Q	flow rate per vertical row of Raschig rings ($\text{m}^3 \text{ s}^{-1}$)
f	fraction of total flow by-passing the annular gap between adjacent Raschig rings	v	volume of annular gap between adjacent Raschig rings in a vertical row (m^3)
		V	superficial velocity of electrolyte (m s^{-1})
		ϕ_A	anodic potential (V)
		ϕ_C	cathodic potential (V)

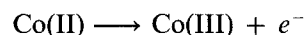
1. Introduction

The use of metal ion catalysts for the oxidation of aromatic hydrocarbons is well established and the industrial possibilities of the technique have been surveyed by Sheldon and Kochi [1]. There is a variety of such ions, but the particular importance of the $\text{Co}^{3+}/\text{Co}^{2+}$ and $\text{Mn}^{3+}/\text{Mn}^{2+}$ systems has been highlighted by the development of the Mid Century Process [2] and similar routes [3] for the production of terephthalic acid from p-xylene.

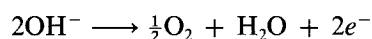
The cobalt system is used in the form of its acetate

and the cobaltic ion can be regenerated from the cobaltous ion by common oxidizing agents such as ozone [4], perchloric acid [5], lead(IV) acetate [6] and perbenzoic acid [7]. More attractively, however, it can be regenerated electrolytically [8], thereby obviating the use of additional chemicals.

The regenerative oxidation occurs at the anode according to the reaction

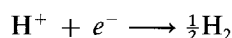
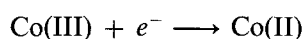


As a competing reaction oxygen is evolved



* Author to whom all correspondence should be addressed.

If an undivided cell is used the reaction occurring at the cathode is



The earliest studies on the electrochemical generation of Co(III) acetate from Co(II) acetate date back to 1952 and were due to Sharp and White [8, 9], who employed a system comprising 95% acetic acid and 5% water, a platinum anode and a copper cathode. The current efficiencies obtained were very low, being for example only 2.1% at 100 A m^{-2} . Recently, however, it was demonstrated [10] that, by replacing platinum with graphite, a much improved performance is achieved. Using a bench scale stirred tank cell with a graphite cloth anode, ceramic divider and graphite rod cathode current efficiencies of 75% were obtained at current densities up to 55 A m^{-2} . In the light of these results further studies [11] were carried out using a frame cell of filter press type, comprising graphite electrodes and a membrane separator. A combination of wide inter-electrode gap, about 20 mm, and a high electrolyte resistivity, in the region of $2 \Omega \text{ m}$, limited current densities to 50 A m^{-2} , however, and resulted in a high specific power consumption.

One means of shortening the inter-electrode gap is to use a bipolar packed bed cell, either in flooded or trickle mode. Such cells can be constructed with gaps of the order of 1 mm and are particularly appropriate in the present case, firstly, because the high resistivity of the electrolyte favours a low level of by-pass current and, secondly, because preliminary cyclic voltammetry had shown that only a small portion of the Co(III) produced at the anodic surfaces is back reduced at the cathodic surfaces. It was felt, therefore, that this type of system was sufficiently promising to warrant further investigation, and the present paper describes studies carried out with a packed bed of graphite Raschig rings operated in a trickle flow mode.

2. Experimental details

2.1. Materials

The materials used were Glacial acetic acid (Merck analytical grade), Cobaltous acetate (BDH, described as $(\text{CH}_3\text{CO}_2)_2\text{Co} \cdot 4\text{H}_2\text{O}$ and confirmed by analysis), and anhydrous sodium acetate (Merck analytical grade). All were used as supplied. The electrolyte comprised a 0.3 M solution of sodium acetate in a 90% acetic acid/water mixture (by volume), with 0.05 M or 0.1 M Co(II) as required.

2.2. Analysis

[Co(III)] was routinely determined by titration with aqueous sodium thio sulphate using starch as indicator, but the results were checked from time to time by u.v. spectrophotometry.

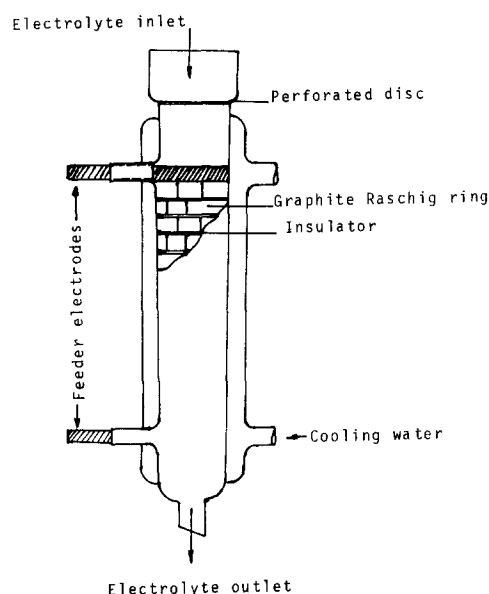


Fig. 1. Bipolar trickle tower.

2.3. Experimental equipment

The experiments were carried out using a bipolar trickle tower, operated as a continuous flow cell as shown in Fig. 1. The tower, of 22 mm internal diameter, was packed with 30 layers of $6 \text{ mm} \times 6 \text{ mm}$ graphite Raschig rings, each layer being separated from the next by a thin disc of polyester mesh. Power from a 300 V/5 A d.c. source was supplied to and

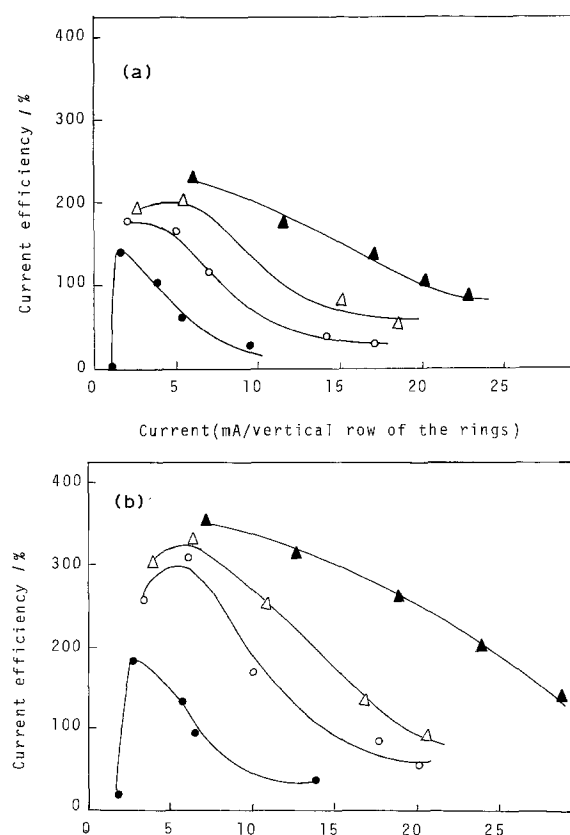


Fig. 2. Variation of current efficiency with current per vertical row of rings for a range of superficial velocities. (a) $[\text{Co(II)}] = 50 \text{ mol m}^{-3}$, $V/\text{m s}^{-1}$: (b) $[\text{Co(II)}] = 100 \text{ mol m}^{-3}$, $V/\text{m s}^{-1}$: (●) 6.7×10^{-5} and (△) 2.0×10^{-4} ; (○) 1.34×10^{-4} and (▲) 4.0×10^{-4} .

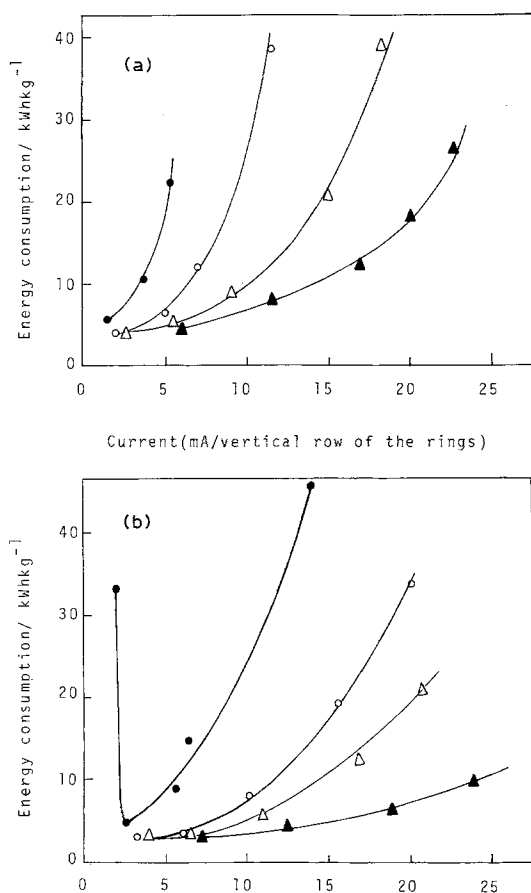


Fig. 3. Variation of the energy consumption with current per vertical row of rings for a range of superficial velocities. (a) $[\text{Co(II)}] = 50 \text{ mol m}^{-3}$, $V/\text{m s}^{-1}$; (b) $[\text{Co(II)}] = 100 \text{ mol m}^{-3}$, $V/\text{m s}^{-1}$: (●) 6.7×10^{-5} and (△) 2.0×10^{-4} ; (○) 1.34×10^{-4} and (▲) 4.0×10^{-4} .

withdrawn from the cell by graphite rods which made contact with the top and bottom layers, the top layer being rendered anodic. Electrolyte was distributed to the top layer via a perforated ceramic disc. The tower was jacketed so that the contents of the column could be maintained at 15°C by passage of cooling water. Low flow rates were obtained by gravity feed, and the higher rates with a peristaltic pump.

2.4. Experimental procedure

The required flow rate was set and the current was then supplied to the cell. The product was collected over a period of half an hour, and analysed. Runs were carried out for a number of flow rates and a range of cell currents.

3. Results

Conversions were determined for two feed concentrations of Co(II) , 0.05 and 0.1M, with cell currents ranging from 1.0×10^{-3} to $27.5 \times 10^{-3} \text{ A/vertical row}$, and flow rates from 8.32×10^{-9} to $5.0 \times 10^{-8} \text{ m}^3 \text{ s}^{-1}$. In presenting the results, flow rate has been converted to a superficial velocity, V , calculated by dividing the volumetric flow rate to each vertical row of rings by the cross sectional area of column occupied by one ring. In this arrangement each ring

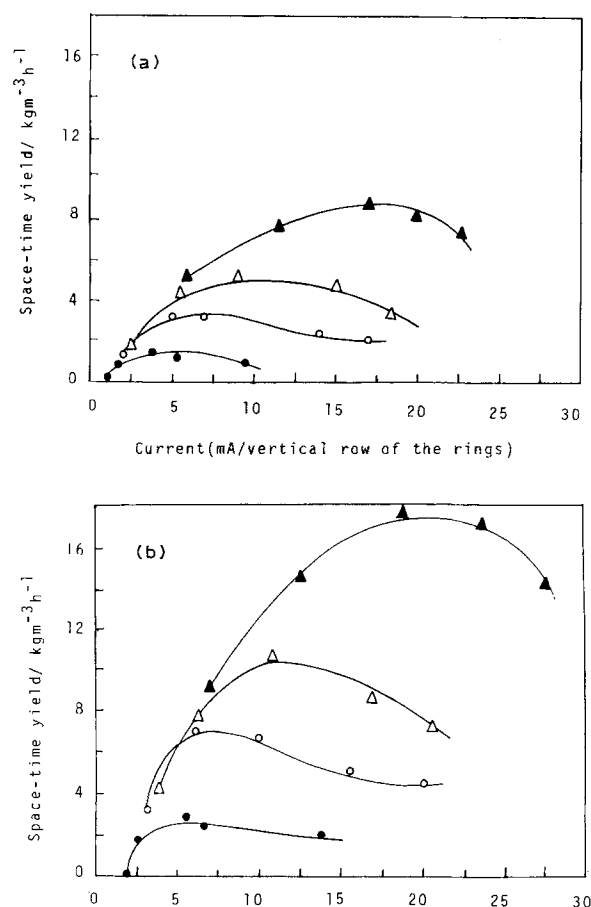


Fig. 4. Variation of space-time yield with current per vertical row of rings for a range of superficial velocities. (a) $[\text{Co(II)}] = 50 \text{ mol m}^{-3}$, $V/\text{m s}^{-1}$; (b) $[\text{Co(II)}] = 100 \text{ mol m}^{-3}$, $V/\text{m s}^{-1}$: (●) 6.7×10^{-5} and (△) 2.0×10^{-4} ; (○) 1.34×10^{-4} and (▲) 4.0×10^{-4} .

occupies a plan area of 0.312 cm^2 and a volume of 0.187 cm^3 . The latter value was employed in the determination of space time yields.

The results are presented in Figs 2 to 4. Figure 2 shows how the observed current efficiency varies with the current supplied to each vertical row of rings for a range of superficial velocities. The current efficiency is based on the current supplied to the cell and, therefore, takes no account of its repeated Faradaic function as it passes from ring to ring. If therefore the anodic process were 100% efficient and there were no back reduction the device as described would offer a maximum current efficiency of 3000%. The values in Fig. 2, ranging as they do from 15 to 350% fall well short of this ceiling.

An obvious feature of both sets of curves in Fig. 2 is that current efficiency displays a clear maximum which, in all cases, corresponds roughly to the same cell current, approximately 6 mA/vertical row of rings. This behaviour is echoed in Fig. 3 where the fall in current efficiency beyond the peak value is the underlying reason for the sharp rise in energy consumption, per kg of product, with increase in current.

From Fig. 3 it is seen that values of energy consumption lie between 3 and 50 kWh per kg of Co(III) for a range of current of 1×10^{-3} to $27.5 \times 10^{-3} \text{ A/vertical row}$. Assuming that the active electrode surface is confined to the plane annular ends of the rings,

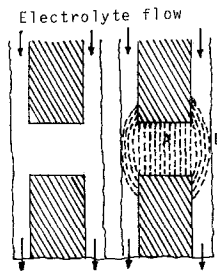


Fig. 5. Possible paths for current flow across the gap between adjacent rings.

these currents represent true current densities of between 200 to 1000 A m^{-2} . If current densities in this range were employed in a narrow gap plate and frame cell, with similar voltage drops, energy consumptions, of 1.5 to 3.5 kWh kg^{-1} would be expected. These values, which are very much lower than those observed in the trickle bed, are based on a current efficiency of 80% and a mass transfer coefficient of 10^{-5} m s^{-1} , which is average for such a cell fitted with a mesh turbulence promoter.

A similar picture emerges when comparison is made on the basis of space time yield, which for the trickle tower varies with current per vertical row according to Fig. 4. The maximum value achieved was $18.08 \text{ kg m}^{-3} \text{ h}^{-1}$ and corresponded to a current of 18.75 mA/vertical row and a superficial velocity of $4 \times 10^{-4} \text{ m s}^{-1}$. An undivided plate and frame cell, with an anode area of typically $20 \text{ m}^2 \text{ m}^{-3}$, operating with an identical true current density (747 A m^{-2}) and a current efficiency of 80% would give a space time yield of $27.7 \text{ kg m}^{-3} \text{ h}^{-1}$, which represents an improvement of more than 50% despite the fact that the trickle tower offers an anode area of $134 \text{ m}^2 \text{ m}^{-3}$. In order to find a possible reason for the less than expected performance of the trickle tower a mathematical model was developed.

4. Mathematical model

The model combines descriptions of both current flow and electrolyte flow. Possible paths for current flow across the gap between adjacent rings is shown in

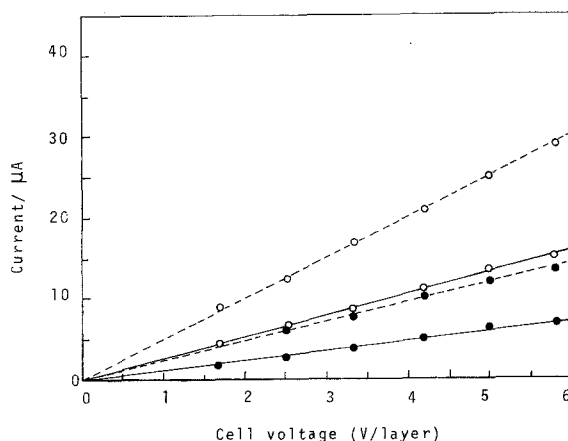


Fig. 6. Variation of bypass current with applied cell voltage. V/m s^{-1} : (●) 6.7×10^{-5} and (○) 4.0×10^{-4} . (—) Co(II) = 50 and (---) Co(II) = 100 mol m^{-3} .

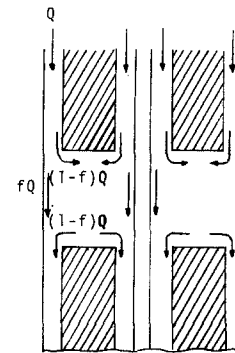


Fig. 7. Electrolyte flow pattern in a trickle tower.

Fig. 5. Path A is directly across the gap between opposing plane annular surfaces and represents the shortest path through the electrolyte, whereas B, which runs between the vertical surfaces, is somewhat longer. Preliminary calculations showed that due to the high resistivity of the electrolyte ($2.2 \Omega \text{ m}$) the bulk of the current would follow path A. This was in line with observations made on a trickle tower comprising glass Raschig rings which were carried out to determine the magnitude of the cell by-pass current. The results are presented in Fig. 6, where it can be seen that the observed currents were in the order of microamps and represented only a fraction of a per cent of the currents supported by the graphite trickle tower with the same cell voltage. For the purposes of the model, therefore, path B was ignored and the active electrode surfaces were regarded as being confined to the opposing planar ends of adjacent rings.

Electrolyte flow down the column was modelled on the basis of the flow pattern presented in Fig. 7. The total volumetric flow rate in the film is Q , of which a fraction $(1 - f)$ passes into the gap between adjacent rings, and is matched by an equal flow out, and the remaining fraction, f , by-passes it. The gap, therefore, is analogous to a continuous stirred tank reactor with by-pass, and can be depicted by Fig. 8, which represents conditions existing in the gap between rings i and $i + 1$. The volume of the 'tank', v , is equal to that of the gap between adjacent rings, and the area of the electrodes, a , is equal to that of the plane ends of the rings. The current flow between the rings is I .

A steady state mass balance on the 'reactor' for species Co(III) is formulated by equating the rate of

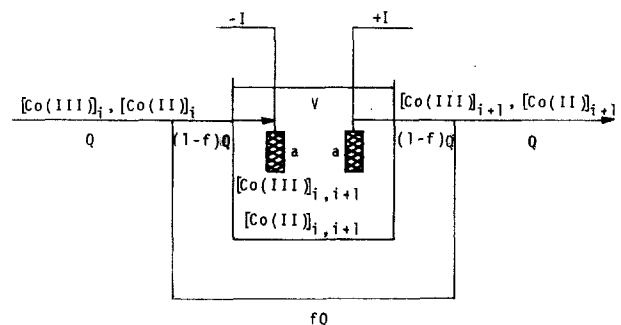


Fig. 8. An ideal continuous stirred tank reactor with bypass as an analogue for the conditions at the gap bounded by rings i and $i + 1$.

flow of Co(III) into the reactor and its rate of production, r_A , at the anode to the rate at which it flows out of the reactor and the rate at which it is destroyed, r_C , at the cathode. Algebraically, this gives

$$(1 - f)Q[\text{Co(III)}]_i + r_A = (1 - f)Q[\text{Co(III)}]_{i+1} + r_C \quad (1)$$

where $[\text{Co(III)}]_i$ is the concentration of cobaltic ion in the film of electrolyte approaching the gap between the rings, and $[\text{Co(III)}]_{i+1}$ is that within the gap. If $i_A(\text{Co})$ and $i_C(\text{Co})$ denote the partial current densities associated with the oxidation of Co(II) and the back reduction of Co(III), respectively, then r_A and r_C can be expressed by

$$r_A = ai_A(\text{Co})/F \quad (2)$$

$$r_C = ai_C(\text{Co})/F \quad (3)$$

Provided the electrode kinetics of the oxidation and reduction reactions can be represented by Tafel relationships the following well established expressions for $i_A(\text{Co})$ and $i_C(\text{Co})$ apply.

$$i_A(\text{Co}) = \frac{F[\text{Co(II)}]_{i,i+1}}{(1/k_L) + (1/k_A \exp(b_A \phi_A))} \quad (4)$$

$$i_C(\text{Co}) = \frac{F[\text{Co(III)}]_{i,i+1}}{(1/k_L) + (1/k_C \exp(-b_C \phi_C))} \quad (5)$$

where k_L is the mass transfer coefficient associated with the transport of cobalt ions from the bulk of the electrolyte occupying the gap between the rings to the upper and lower annular surfaces enclosing the gap. Its value is assumed to be the same for both Co(II) and Co(III) ions. The parameters k_A and k_C are the rate constants for the oxidation of Co(II) and the reduction of Co(III), respectively, b_A and b_C the exponential constants and ϕ_A and ϕ_C are the anodic and cathodic potentials.

To obtain a closed set of equations expressions for the partial current densities associated with the competitive secondary reactions must be included. These reactions arise from the breakdown of the solvent and give rise to oxygen evolution at the anode and hydrogen evolution at the cathode. Since the solvent was present in high concentration and the current densities employed were relatively low and the mass transfer resistance with respect to solvent breakdown was ignored and the secondary partial current densities was expressed by

$$i_A(\text{O}) = k_O \exp(b_O \phi_A) \quad (6)$$

$$i_C(\text{H}) = k_H \exp(-b_H \phi_C) \quad (7)$$

Since the solvent composition was not a variable and was virtually unaffected by the electrolysis the concentration terms normally present in Equations 6 and 7 have been subsumed in the constants k_O and k_H .

If I is the cell current per column of rings, a coulombic balance gives

$$I = a(i_A(\text{Co}) + i_A(\text{O})) \quad (8)$$

$$I = a(i_C(\text{Co}) + i_C(\text{H})) \quad (9)$$

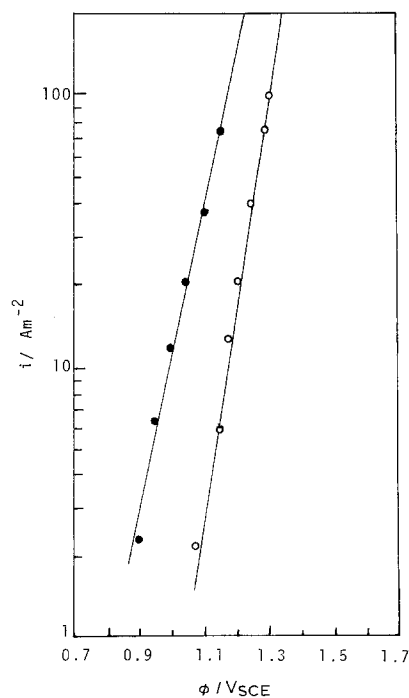


Fig. 9. Polarization curves for the relevant anodic reactions. $[\text{Co(II)}] = 0.05 \text{ M}$, $[\text{sodium acetate}] = 0.30 \text{ M}$ in 90% acetic acid/10% water by volume. (O) $\text{H}_2\text{O} \rightarrow \frac{1}{2}\text{O}_2 + 2\text{H}^+$ and (●) $\text{Co}^{2+} \rightarrow \text{Co}^{3+}$. RDE speed = 1000 r.p.m.

Values of the kinetic constants k_A , k_C , k_O , k_H , b_A , b_C , b_O and b_H were determined from preparative and polarization experiments using a graphite rotating disc electrode. Ohmic corrections for the potential drop between luggin tip and disc, which could not be ignored in this case, were determined by momentarily interrupting the current using a logic switch and recording the time decay of potential on a digital storage oscilloscope transient recorder (Gould type 1425). Data from which the kinetic constants were determined are presented in Figs 9 and 10 and their values are as follows:

$$k_A = 4.64 \times 10^{-7} \quad k_C = 3.73 \times 10^{-3} \text{ A m mol}^{-1}$$

$$k_O = 6.09 \times 10^{-9} \quad k_H = 0.912 \text{ A m}^{-2}$$

$$b_A = 13.08 \quad b_C = -13.69 \text{ V}^{-1}$$

$$b_O = 18.31 \quad b_H = -11.68 \text{ V}^{-1}$$

The values are appropriated to ϕ being measured in volts with respect to SCE.

The concentrations $[\text{Co(III)}]_{i+1}$ and $[\text{Co(II)}]_{i+1}$ in the electrolyte film flowing over ring $i + 1$ are obtained by carrying out a mass balance at the point where the exit stream from the gap re-combines with the bypass stream, giving

$$[\text{Co(III)}]_{i+1} = (1 - f)[\text{Co(III)}]_{i,i+1} + f[\text{Co(III)}]_i \quad (10)$$

$$[\text{Co(II)}]_{i+1} = (1 - f)[\text{Co(II)}]_{i,i+1} + f[\text{Co(II)}]_i \quad (11)$$

A final restriction on the system is set by the condition

$$[\text{Co(III)}] + [\text{Co(II)}] = \text{constant} \quad (12)$$

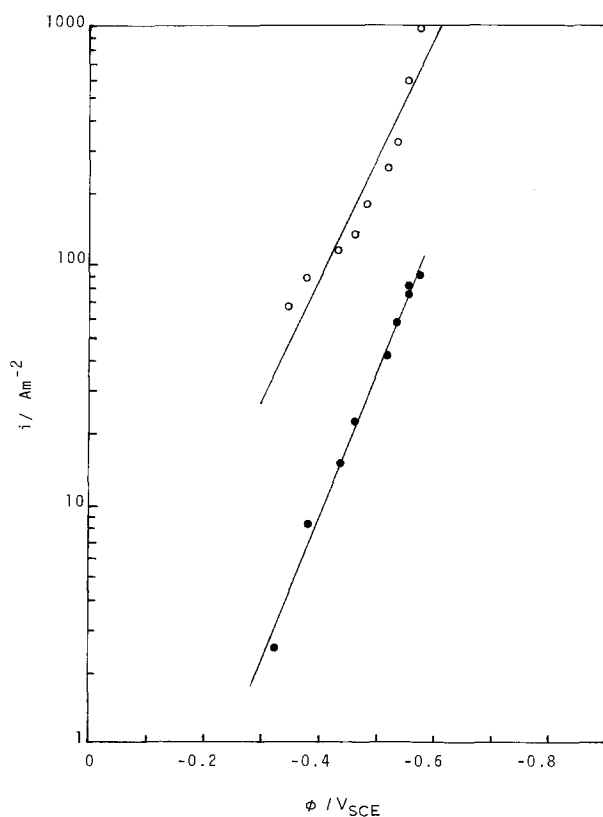


Fig. 10. Polarization curves for the relevant cathodic reactions. $[\text{Co(III)}] = 0.05 \text{ M}$, $[\text{sodium acetate}] = 0.30 \text{ M}$ in 90% acetic acid/10% water by volume. (O) $\text{H}^+ \rightarrow \frac{1}{2}\text{H}_2$ (●) $\text{Co}^{3+} \rightarrow \text{Co}^{2+}$. RDE speed = 1000 r.p.m.

The 'constant' in the present context being equal to the feed concentration of Co(II).

These equations were solved numerically, progressing from $i = 1$ to 30 to give, finally, a value for $[\text{Co(III)}]_{31}$, the concentration of cobaltic ion at the reactor exit.

To initiate the calculations the process conditions of interest were specified, these being the concentrations of cobaltous and cobaltic ions in the feed, $[\text{Co(II)}]_i$ and $[\text{Co(III)}]_i$, the volumetric flow rate, Q , and the reactor current, I , both of the latter being with respect to

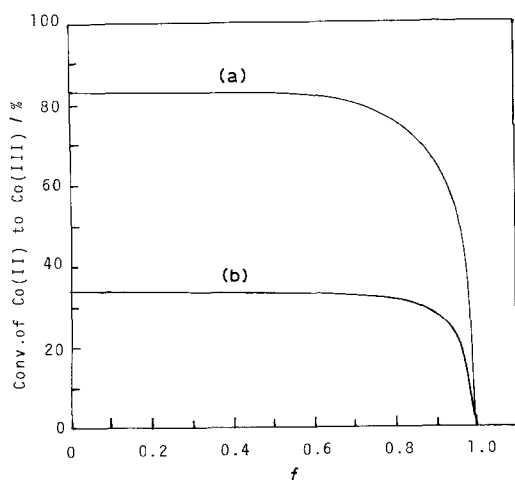


Fig. 11. Effect of f on conversion. (a) Absence of mass transfer resistance, k_L infinite; (b) $k_L = 1.0 \times 10^{-5} \text{ ms}^{-1}$; $\text{Co(II)} = 100 \text{ mol m}^{-3}$; $V = 4.0 \times 10^{-4} \text{ m s}^{-1}$; and $I = 7 \text{ mA/vertical row}$.

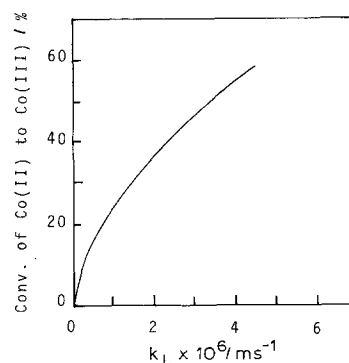


Fig. 12. Effect of mass transfer coefficient on conversion. $[\text{Co(II)}] = 100 \text{ mol m}^{-3}$; $V = 6.7 \times 10^{-5} \text{ m s}^{-1}$; and $f = 0.5$.

one vertical row of rings. Values of k_L and f were also required. Since, however, these parameters are unknown functions of the hydrodynamic, geometric and physical properties of the system they were in fact treated as tuning variables for matching the model to observation.

The sequence of the calculations used in solving Equations 1 to 12 for any particular value of i was as follows. A value for $[\text{Co(III)}]_{i,i+1}$, was first guessed, which from Equation 12, gave a corresponding value of $[\text{Co(II)}]_{i,i+1}$. A value of ϕ_A was guessed from which, using Equations 4 and 6, values of $i_A(\text{Co})$ and $i_A(\text{O})$ were calculated. Their sum was then compared with I according to the requirement of Equation 8, ϕ_A being iterated until equality was reached. Identical calculations were then carried out for ϕ_C . The final values of ϕ_A and ϕ_C were then used to determine $i_A(\text{Co})$ and $i_C(\text{Co})$ from Equations 4 and 5, thereby yielding r_A and r_C from Equations 2 and 3 and finally $[\text{Co(III)}]_{i,i+1}$ from Equation 1. This value was compared with the initial guess, and iterative calculations were carried out until agreement was reached. When this was achieved $[\text{Co(III)}]_{i+1}$ was determined from Equation 10 and $[\text{Co(II)}]_{i+1}$ from Equation 12. These latter values then provided the initial concentrations for gap $(i + 1, i + 2)$. Starting from the first gap and applying this procedure consecutively to all the gaps in the vertical row of rings, the concentration of Co(III) in the electrolyte leaving the cell was determined. Simple calculations then allowed other quantities, such as current efficiency, to be evaluated.

In matching the model to observation its sensitivity to variation in f , the hydrodynamic by-pass, was first examined, and Fig. 11 shows the calculated effect of f on conversion for typical column conditions both in the absence of mass transfer resistance and when the mass transfer coefficient is $1.0 \times 10^{-5} \text{ m s}^{-1}$. In both cases it is seen that bypass has relatively little effect on column performance unless it reaches values in excess of 90%, which seems unlikely. The effect of mass transfer coefficient, k_L , on the other hand, was much more emphatic. A typical curve showing the variation of conversion with k_L for a fixed value of f is presented in Fig. 12, from which it is seen that column performance is characterized by a steep and steady decline as k_L falls from 6.0×10^{-6} to $1.0 \times 10^{-6} \text{ m s}^{-1}$, a

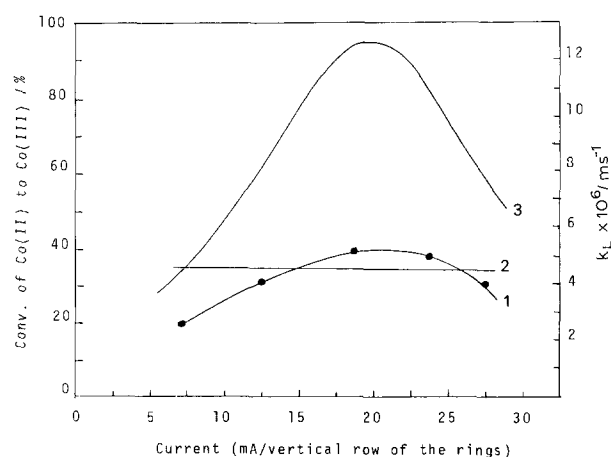


Fig. 13. Comparison of the variation of conversion with current observed experimentally with that predicted by the model. (1) Experimental results; (2) theoretical results, $k_L = 1.0 \times 10^{-5} \text{ m s}^{-1}$; (3) variation of mass transfer coefficient required by the model for the simulation of curve 1; $[\text{Co(II)}] = 100 \text{ mol m}^{-3}$; $V = 4.0 \times 10^{-4} \text{ m s}^{-1}$; and $f = 0$.

reasonable range of values for the laminar flow conditions which are almost certainly obtained in the trickle tower. From these calculations it was deduced, that a lack of a good mass transfer environment in the gaps rather than hydrodynamic bypass, was the cause of the reduced performance of the column in comparison to a plate and frame device.

Attempts to obtain a close match between the model and observed results were not entirely successful. For example Fig. 13 compares the variation of conversion with current observed experimentally (curve 1) for a superficial velocity of $4 \times 10^{-4} \text{ m s}^{-1}$, with that predicted by the model (curve 2) using a mass transfer coefficient of $1.0 \times 10^{-5} \text{ m s}^{-1}$. The experimental results show a pronounced maximum whereas the predicted results are almost uniformly level. To mimic this maximum the model demands a variable mass transfer coefficient changing as depicted by the third curve in Fig. 13. This shows that as the current rises to 18 mA/vertical row the coefficient would have to increase from about $4 \times 10^{-6} \text{ m s}^{-1}$ to a maximum of $12.5 \times 10^{-6} \text{ m s}^{-1}$, falling back to $8 \times 10^{-6} \text{ m s}^{-1}$ as the current is raised to 27 mA/vertical row.

Despite the fact that the results under discussion are for constant flow rate, a possible change in mass transfer coefficient is not entirely inexplicable. The initial rise, for instance, may be due to greater agitation accompanying the increased gassing at the electrodes, whereas the fall at higher currents may reflect not so much a change in mass transfer coefficient as a reduced surface area due to gas bubble build-up. In addition, the model itself is conceptually simple and some aspects of the observed behaviour of the column may arise from phenomena which have been ignored

by the model. For instance by equating the gap to an ideal CSTR no attempt has been made to take into account any imperfection in mixing there, a condition which would almost certainly be affected by gas evolution.

5. Conclusion

Although a trickle tower of graphite Raschig rings is attractive in that it is a relatively simple and inexpensive form of electrolytic cell, its use in the production of Co(III) ions from Co(II) ions using the cobaltous acetate-sodium acetate-acetic acid system has been shown to be relatively inefficient.

Its performance quickly reaches a maximum with increase in current, resulting in energy consumption in excess of $3\text{--}5 \text{ kWh kg}^{-1}$ for space time yields of only $6\text{--}8 \text{ kg m}^{-3} \text{ h}^{-1}$ of Co(III). This compares with an expected performance of say 5 kWh kg^{-1} and a space time yield of perhaps $20 \text{ kg m}^{-3} \text{ h}^{-1}$ for a plate and frame cell. It is suggested that the inefficiency derives from the fact that the active electrode surfaces are largely confined to the opposing annular edges of adjacent Raschig rings where conditions for good mass transport are unfavourable. On these grounds it is felt that a rod cell [12] operated in the flooded mode would, in the present context, be a more useful device. Such a cell is capable of much higher mass velocities with virtually no hydrodynamic by-pass, thereby creating conditions conducive to greatly improved mass transfer rates.

Acknowledgement

The majority of this work was carried out in the Department of Chemical Engineering, University of Newcastle upon Tyne. The authors wish to thank Anadolu University and the British Council for support.

References

- [1] R. A. Sheldon and J. K. Kochi, 'Metal Catalysed Oxidations of Organic Compounds', Academic Press, New York (1981).
- [2] R. Landau and A. Saffer, *Chem. Eng. Prog.* **64** (1968) 20.
- [3] P. H. Towle and R. H. Baldwin, *Hydrocarbon Process* **43** (1964) 149.
- [4] A. Hay, J. Eustance and H. Blanchard, *J. Org. Chem.* **25** (1960) 616.
- [5] E. Koubek and J. O. Edwards, *J. Inorg. Nucl. Chem.* **25** (1963) 1401.
- [6] D. Benson, J. Prall, L. Sutcliffe and J. Walkley, *Discuss. Faraday Soc.* **60** (1960) 201.
- [7] R. A. Sheldon and J. K. Kochi, *Adv. Catalysis* **25** (1976) 295.
- [8] J. A. Sharp and A. G. White, *J. Chem. Soc.* (1952) 110.
- [9] J. A. Sharp and A. G. White, *ibid.* (1957) 2030.
- [10] U. Bakir Ogutveren and A. T. Pekel, *B. Electrochem.* **5** (1989) 452.
- [11] Z. Poyraz, Masters thesis, Anadolu University (1983).
- [12] F. Goodridge, C. J. H. King and A. R. Wright, *Electrochim. Acta* **22** (1977) 347.